J Mater Sci: Mater Med (2008) 19:2445–2452
DOI 10.1007/s10856-008-3366-9

Fabrication and characterization of porous poly(L-lactide) scaffolds using solid–liquid phase separation

Yan Qi Goh · Chui Ping Ooi

Received: 26 June 2007 / Accepted: 2 January 2008 / Published online: 25 January 2008

Abstract Freeze-extraction, which involves phase separation principle, gave highly porous scaffolds without the time and energy consuming freeze-drying process. The presented method eliminates the problem of formation of surface skin observed in freeze-drying methods. The effects of different freezing temperature (−80 and −24°C), medium (dry ice/ethanol bath and freezer) and polymer concentrations (1, 3, and 5 wt.%) on the scaffold properties were investigated in connection with the porous morphology and physicomechanical characteristics of the final scaffolds. The FESEM micrographs showed porous PLLA scaffolds with ladder-like architecture. The size of the longitudinal pores was in the range of 20–40 μm and the scaffolds had high porosity values ranging from 90% to 98%. Variation in porosity, mechanical resistance, and degree of regularity in the spatial organization of pores were observed when polymer concentration was changed. More open scaffold architecture with enhanced pore interconnectivity was achieved when a dry ice/ethanol bath of −80°C was used. Polymer concentration played an important role in fabricating highly porous scaffolds, with ladder-like architecture only appearing at polymer concentrations of above 3 wt.%. With the freeze-extraction method used here, highly porous and interconnected poly(L-lactide) scaffolds were successfully fabricated, holding great potential for tissue engineering applications.

Y. Q. Goh · C. P. Ooi (✉)
Division of Bioengineering, School of Chemical and Biomedical Engineering, Nanyang Technological University, Nanyang Avenue, Singapore 639798, Singapore
e-mail: ascpooi@ntu.edu.sg

1 Introduction

Tissue engineering is "an interdisciplinary field that applies the principles of engineering and life sciences toward the development of biological substitutes that restore, maintain, or improve tissue function or a whole organ" [1]. It is an alternative to organ transplantation, which faces the critical problem of shortage in organ donors.

Porous scaffolds have been used as a template for the attachment of cells so that the cells are guided and able to proliferate, differentiate, and secrete extracellular matrix (ECM) [2–4]. As a result, functional tissues and organs could then be obtained and applied to tissue engineering purposes. Numerous methods have been employed to fabricate scaffolds. They include solvent casting/particulate leaching [5, 6], phase separation/emulsification [7–12], fiber bonding [13, 14], gas foaming [15, 16], and 3D-printing [17, 18]. A combination of different techniques has also been reported to yield scaffold of enhanced characteristics [19, 20]. Scaffold design is essentially very important so that transplanted cells are able to survive, adhere, and retain their ability to proliferate, migrate, and differentiate within the scaffold [21]. The importance of desired pore size in bone formation was demonstrated by Pineda et al. [22] and Brauker et al. [23]. Porosity would also affect both the amount of cells and matrix formed within the construct, as well as the structure of this newly formed tissue. High porosity of scaffolds enhanced cell infiltration and proliferation as reported by Gomes et al. [24].

Thermally induced phase separation (TIPS) to create porous scaffolds is gaining attention recently. It requires the temperature of the polymer solution to be lowered to bring about phase separation into polymer-rich and

polymer lean phases. Solvent which is in the polymer-lean phase will then be removed through extraction, evaporation, or sublimation, giving rise to the pores of the scaffolds. It is a rather complicated process as it involves the thermodynamics and kinetic behavior of the polymer solution under the processing conditions. There are two kinds of polymer phase separation technique: (i) solid–liquid phase separation and (ii) liquid–liquid phase separation. For solid–liquid phase separation, temperature is lowered to freeze a polymer solution. The solvent in the system will form crystals and polymer is separated from the solvent crystallization front. Subsequent removal of solvent crystals gives rise to pores in the scaffolds. Liquid–liquid phase separation, on the other hand, generates polymer-rich and polymer-poor liquid phases. Polymer-poor phase is developed further to form the pores in the scaffolds. Most of the phase separation methods require the use of a freeze-dryer to remove the solvent, which is very time and energy consuming, and takes from several days up to a period of 2 weeks to produce a scaffold [7–11]. There is also the formation of surface skin, which appears after the evaporation of solvent. A more efficient method was reported by Ho et al. [12], where the solvent was removed with ethanol aqueous solution, resulting in similar pore structure without the surface skin.

Here, porous PLLA scaffolds were successfully created with the use of ethanol aqueous solution without the use of a freeze-dryer. Fabrication parameters, which included the freezing temperature, freezing medium, and the polymer concentration, were varied accordingly. The morphology and the physicochemical characteristics of scaffolds fabricated through this freeze-extraction technique in relations to these fabrication parameters are discussed.

2 Experimental

2.1 Materials

Purasorb® Poly(L-lactide), PLLA with inherent viscosity of 1.2 dl/g, M_w of 130,000 Da was purchased from Purac. 1,4-dioxane of ReagentPlus® Grade, ≥99% purity, was purchased from Sigma Aldrich Pt Ltd. Ethanol of analytical grade was purchased from Sino Chemical Company Pt Ltd.

2.2 Preparation of PLLA scaffolds

PLLA scaffolds were prepared by varying three conditions: (i) freezing temperature (−80 and −24°C); (ii) freezing medium (dry ice/ethanol bath and freezer), and (iii) polymer concentrations (1, 3, and 5 wt.%). PLLA was first dissolved in 1,4-dioxane to form polymer solutions of desired concentrations (PLLA/1,4-dioxane of 1, 3, and 5 wt.%). The polymer solution was then placed in a glass petridish and frozen at −80 and −24°C using a freezer and at −80°C using a dry ice/ethanol bath. The solvent was then removed using freeze-extraction. The procedure involves immersing the frozen polymer solution into ethanol aqueous solution at a concentration of 80 wt.% and pre-cooled to −24°C for 2 days. The solvent was extracted and replaced with ethanol aqueous solution, which is miscible with 1,4-dioxane and a non-solvent for PLLA. Drying was carried out at room temperature for another 2 days to remove the aqueous ethanol in the polymer matrix. The dried samples were then kept in a dessicator cabinet at 22°C and 40% relative humidity to reduce the absorption of moisture which leads to degradation of the fabricated scaffolds prior to further characterization.

2.3 Characterization of PLLA scaffolds

2.3.1 FESEM analysis

JEOL JSM-6700F, field emission SEM was used to examine the morphologies of the PLLA scaffolds. Prior to FESEM analysis, samples were coated with platinum using a JEOL JFC-1600 Auto Fine Coater operated at 10 mA for 80 s. The longitudinal and transversal sections of the samples were taken for FESEM analysis.

2.3.2 DSC analysis

Thermal properties of the scaffolds were determined through the use of PerkinElmer® Diamond Differential Scanning Calorimeter. A sample weight of approximately 5.5 mg was sealed in an aluminum pan for each run. A blank reference pan was used. A heating rate of 5°C min^{-1} was applied and the sample was heated from 25 to 220°C.

2.3.3 Porosity measurements

The porosity, ε, of PLLA scaffolds was determined as follows. Mass of the fabricated scaffold was first measured with an analytical balance and the volume calculated from the average dimensions of six specimens of each scaffold to obtain an average scaffold density, D_f. From the scaffold density, D_f, and polymer skeletal density, D_p, the porosity, ε, was calculated using Eq. 1:

$$\text{Total porosity, } \varepsilon = \frac{D_p - D_f}{D_p} \times 100\% \quad (1)$$

Polymer skeletal density, D_p, was determined by:

$$D_p = \frac{1}{\frac{1-X_c}{D_a} + \frac{X_c}{D_c}} \quad (2)$$

where the density for completely amorphous PLLA, D_a, is 1.248 g ml^{-1} [7], the density for completely crystalline PLLA, D_c, is 1.290 g ml^{-1} [7], and X_c is the degree of crystallinity computed by Mikos et al. [5] as:

$$X_c = \frac{\Delta H_m}{\Delta H_m^o} \quad (3)$$

where ΔH_m^o is the enthalpy of melting for 100% crystalline PLLA (203.4 J g^{-1}) [5]. This computation for the degree of crystallinity could be utilized as the samples did not exhibit cold crystallization as seen from the DSC thermograms.

2.3.4 *Determination of pore size*

The pore size was estimated from the longitudinal and transversal views of the FESEM micrographs. For the longitudinal pore size, the length of the pore along the longitudinal direction was taken. The transversal pore size was measured using the length of the pores in the transversal views. The average of 10 readings of pore size was taken for each sample.

3 Results and discussion

3.1 Preparation of PLLA foams by freeze-extraction

The freezing point of pure 1,4-dioxane is 11.8°C. As the polymer solutions were quickly transferred to a dry ice/ethanol bath or freezer at a preset temperature of −80 and −24°C, no liquid–liquid phase separation occurred. The solvent crystallized thus inducing solid–liquid phase separation, which was responsible for the highly anisotropic morphology that is dependent on the crystallization mode of the solvent.

A longitudinal cross section through a PLLA-foam prepared from a 5 wt.% solution in 1,4-dioxane shows long-range orientation of well-defined porous channels made of parallel lamellae (Fig. 1a). A higher magnification (Fig. 1b) reveals the regularity and directionality of the pores with the ladder-like substructure of the lamellae. The longitudinal pore size was found to range from 20 to 40 μm, as shown in Fig. 1b. A transverse cross section (Fig. 2) illustrates a series of elongated pores, the length of which was in the range of 100−200 μm. A local temperature gradient from the surface to the center of the polymer solution led to the anisotropic pore structure. Its channels were parallel to the temperature gradient and had repeating

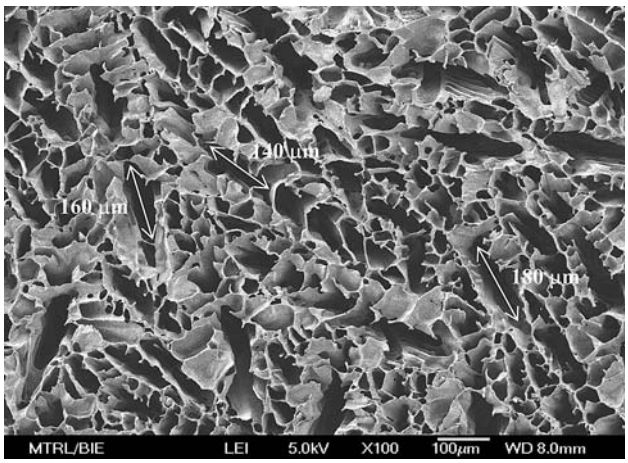

Fig. 2 FESEM transversal section of 5 wt.% PLLA/1,4-dioxane samples using −80°C freezer

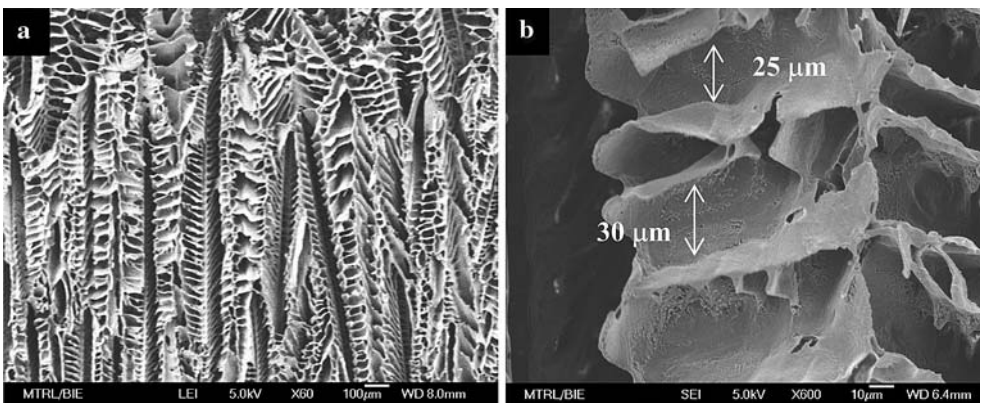

Fig. 1 FESEM longitudinal section of 5 wt.% PLLA/1,4-dioxane samples using −80°C freezer, at (**a**) ×60, (**b**) ×600 magnification

Table 1 Degree of crystallinity and porosity values of PLLA scaffolds fabricated using freeze extraction

Concentration (wt.%)	Freezing temperature (°C)	Freezing medium	Melting temperature (°C)	Degree of crystallinity (%)	Porosity (%)
As-received PLLA	–	–	169.8	18.29	–
5	−24	Freezer	167.4	18.99	89.99
			168.1		
			168.7		
5	−80	Freezer	167.5	18.40	90.01
			169.2		
5	−80	Dry ice/ethanol bath	163.3	17.95	90.82
			168.8		
3	−24	Freezer	168.9	18.84	93.91
3	−80	Freezer	168.6	17.67	94.24
3	−80	Dry ice/ethanol bath	169.3	20.97	95.44
1	−24	Freezer	168.7	18.76	97.97
1	−80	Freezer	168.8	18.53	96.48
1	−80	Dry ice/ethanol bath	168.4	19.08	97.66

partitions with nearly uniform spacing perpendicular to the solidification direction.

The scaffolds were highly porous, with porosity larger than 0.9 (Table 1) and were similar to those fabricated using a freeze-dryer, as reported by Ma et al. [7], Schugens et al. [10], and Tu et al. [11].

3.1.1 *Effect of freezing temperature on scaffold morphology*

Two quenching temperatures were compared in this work. The polymer solutions at 25°C were placed in a freezer at −24 and −80°C for 20 min. The initial quenching rates

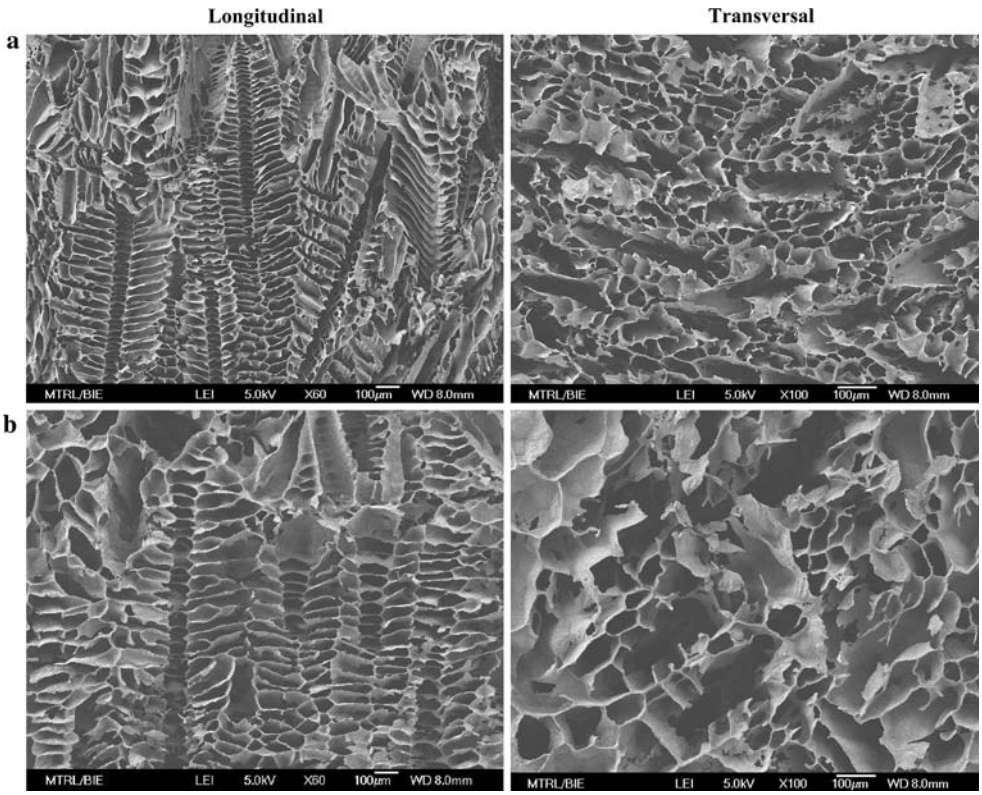

Fig. 3 FESEM micrographs of foams fabricated by freeze-extraction of 3 wt.% PLLA/1, 4-dioxane samples using freezer at (**a**) −80°C and (**b**) −24°C

were 2.5 and 5°C/min, respectively, and were assumed uniform throughout the scaffold. The frozen polymer solution was then immersed in an ethanol aqueous solution that was pre-cooled to −24°C for extraction of solvent. The final morphology of the polymer foams analysed by FE-SEM (Fig. 3) shows a dependence on the initial quenching rate. When a lower freezing temperature of −80°C was used, the foams showed more randomly orientated porous channels compared to foams fabricated at −24°C. Moreover, the ladder-like structure observed at −24°C was more uniform in shape and size and were more orderly arranged when compared with the −80°C samples. The average longitudinal and transversal pore size increase with higher freezing temperature (or slower quenching rate) in the range of polymer concentration used, as observed in Fig. 4(a) and (b). This observation is in agreement with the data reported in scientific literature [25], where the porosity of foams prepared by freeze-drying depends on the quenching rate of the original homogeneous polymer solution, with a faster quenching rate usually resulting in a decrease in average pore size. In the case of slow quenching rate, phase coalescence occurs in order to decrease the interfacial energy. This allows for larger growth of the 1,4-dioxane crystals, which ultimately results in large pores.

The porosity of the scaffolds was not significantly affected by the quenching rate. The constant porosity could be maintained, despite the increase in pore size, by a decrease in nucleation of 1,4-dioxane crystals at −24°C, which would lead to fewer pores formed.

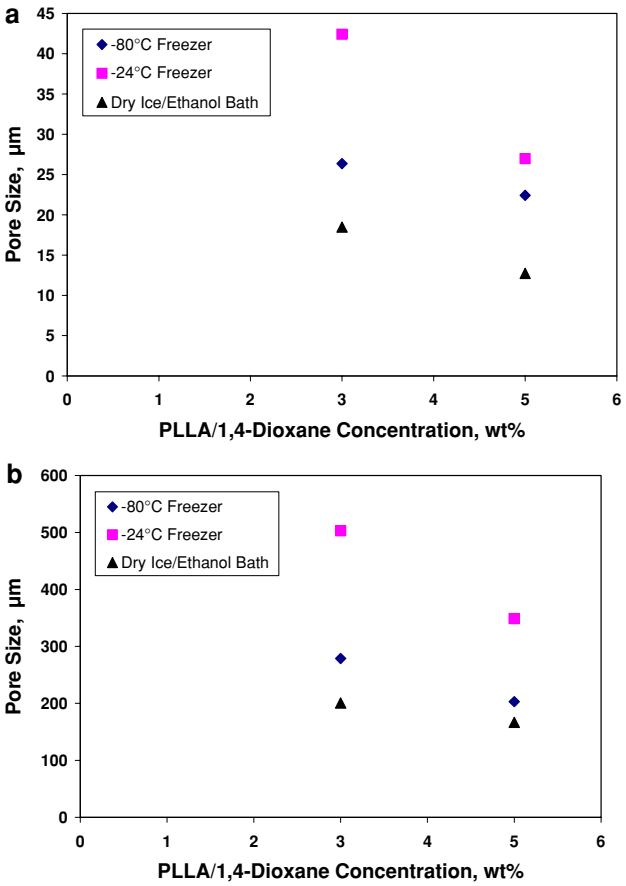

Fig. 4 Effect of temperature, freezing medium, and PLLA/1,4-dioxanane concentration on (**a**) average longitudinal pore size and (**b**) average transversal pore size

3.1.2 Effect of freezing medium on scaffold properties

The overall architecture of the porous scaffold obtained using a dry ice/ethanol bath had porous channels with ladder-like structures that ran longitudinally for all the samples except at 1 wt.% polymer concentration (Fig. 5). Similar structures were observed for scaffolds prepared using a freezer. The significant interesting difference between using a dry ice/ethanol bath and a freezer is that in the former, the ladder-like branches themselves had ladder-like micro-structures (parallel microtubles with thin partitions). This gave the whole structure a more interconnected architecture. Hence, pore interconnectivity within the scaffolds fabricated using the dry ice/ethanol bath was expected to be enhanced. This might induce better cell in-growth throughout the whole porous scaffold. The pore wall was also thinner in scaffolds fabricated using the −80°C dry ice/ethanol bath when compared to scaffolds created using a −80°C freezer. At low polymer concentration of 1 wt.%, micropores were observed on the walls of the scaffolds (Fig. 5).

The average pore size (for both longitudinal and transversal sections) was found to be smaller in scaffolds fabricated using the dry ice/ethanol bath than in the freezer (Fig. 4a and b). As the polymer solution was immersed in the dry ice/ethanol bath, the solution may have a higher degree of super-cooling in the dry ice/ethanol mixture than in the freezer at the same phase-separation temperature (−80°C). This might result in different solvent crystallization kinetics (faster nucleation and slower growth of dioxane crystals in the polymer solution) and therefore the different pore architectures of the porous materials.

The porosity values for both scaffolds were large and in the range of 90–98%. The different freezing mediums influenced the porosity of the scaffolds. The porosity values for scaffolds fabricated using the dry ice/ethanol bath were larger than those from freezer for the various polymer concentrations (Table 1).

3.1.3 Effect of polymer concentration on scaffold properties

Polymer concentration affected the porous structure, where more regular pore architecture was observed in scaffolds

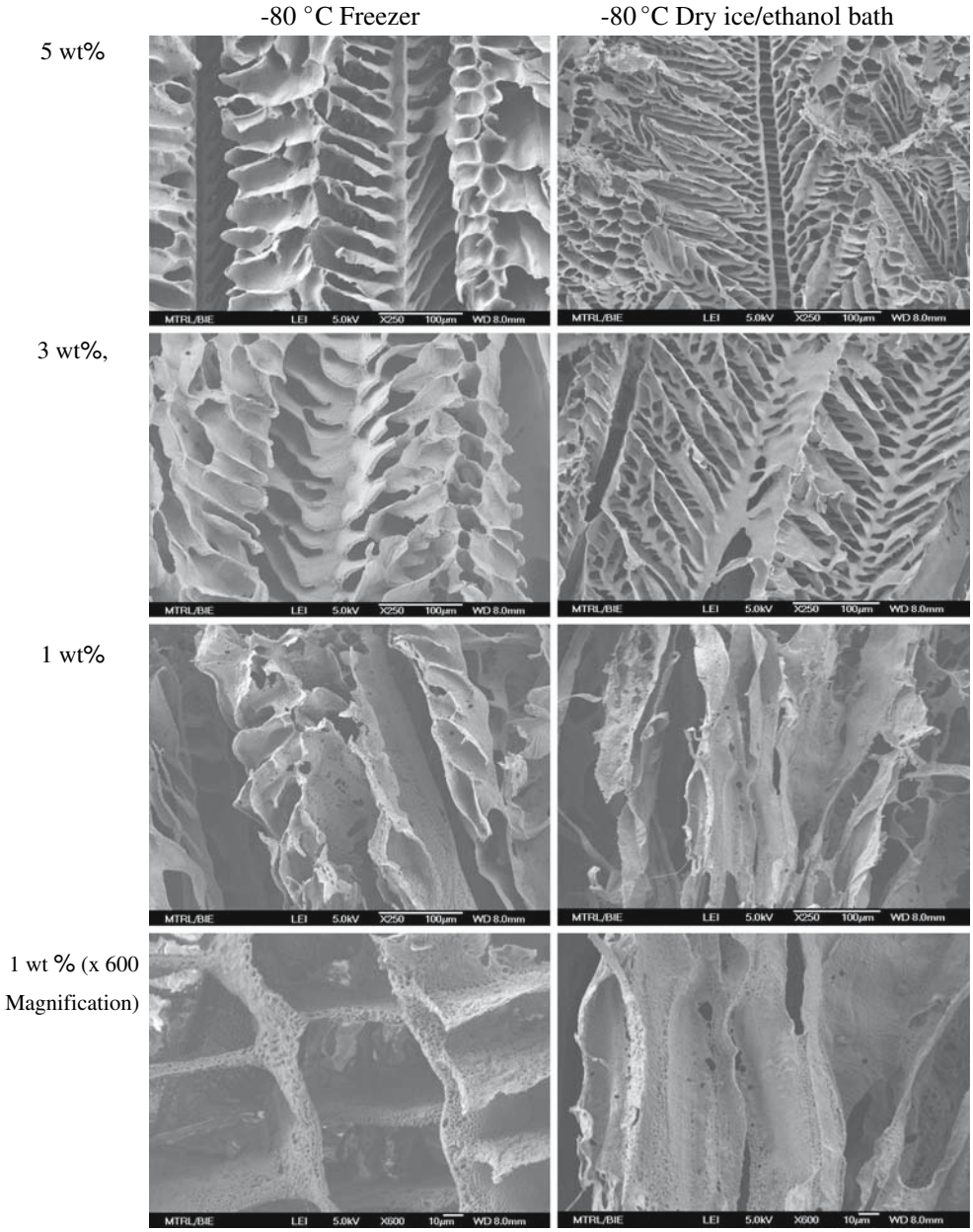

Fig. 5 FESEM micrographs of foams fabricated by freeze-extraction of 5, 3, and 1 wt.% PLLA/1,4-Dioxane at −80°C using a freezer and dry ice/ethanol bath.

prepared from PLLA solution of 5 wt.% than 1 wt.% (Fig. 5). The ladder-like morphology became less defined with lower polymer concentration of 1 wt.%. During the extraction of dioxane from the frozen matrix of 1 wt.% concentration, the lack of polymer material to support the whole structure led to the undefined structure and pores.

The porosity decreased with an increase in the polymer concentration (Table 1) since less solvent phase-separates when a solution of higher PLLA concentration underwent freeze extraction. This corresponded to the decrease in pore size with increase in polymer concentration irrespective of the freezing temperature or mediums used. Since the rate of nucleation remains constant at fixed temperatures, the higher solvent exclusion from the crystalline regions in the higher polymer concentration would account for the decrease in pore size and porosity (Fig. 4 and Table 1).

3.2 Thermal properties of PLLA scaffolds

All the scaffolds showed a melting temperature, T_m, of (168.9 ± 0.4)°C. This melting temperature was similar to

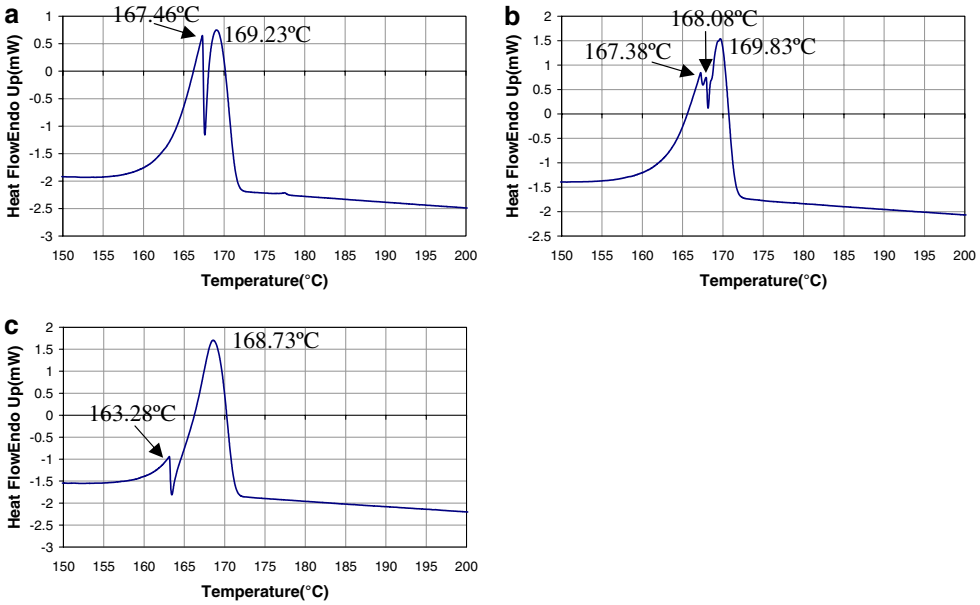

Fig. 6 DSC thermogram showing the peak melting temperature, T_m, of PLLA scaffold fabricated from 5 wt.% PLLA/1,4-dioxane; (**a**) −80°C freezer, (**b**) −24°C freezer, and (**c**) dry ice/ethanol bath (∼−80°C)

Table 2 Mechanical characteristics of PLLA scaffolds prepared by freeze extracting solutions of various concentrations in 1,4-dioxane

Concentration (wt.%)	Freezing temperature (°C)	Freezing medium	Macroscopic aspect	Mechanical behavior	Flexibility
5	−24	Freezer	Rigid foam	Hard-tough	Moderate
	−80	Freezer	Rigid foam	Hard-tough	Moderate
	−80	Dry ice/ethanol	Rigid foam	Hard-tough	Moderate
3	−24	Freezer	Rigid foam	Hard-tough	Low
	−80	Freezer	Rigid foam	Hard-tough	Low
	−80	Dry ice/ethanol	Rigid foam	Hard-tough	Moderate
1	−24	Freezer	Rigid foam	Soft	High
	−80	Freezer	Rigid foam	Soft	High
	−80	Dry ice/ethanol	Rigid foam	Soft	High

the as-received PLLA (Table 1). The polymer crystal size in the scaffolds was similar to the as-received polymer and was unaffected by the different processing parameters used during the fabrication process. The degree of crystallinity, X_c, of the different scaffolds remained unchanged, within experimental error, with respect to different processing parameters. The X_c, calculated was (18.79 ± 0.94)% and was similar to that of as-received PLLA. The PLLA scaffolds retained their semicrystalline morphologies irrespective of the various freezing conditions used during the samples preparation.

Multiple endotherms (Fig. 6) were only observed in the DSC thermograms of 5 wt.% PLLA samples. The presence of multiple peaks in the 5 wt.% PLLA solution may be due to a higher density of smaller PLLA crystal sizes in the more viscous polymer solution. As different crystal sizes may be present in a polymer solution, a higher density of smaller size PLLA crystals will be more observable for a more concentrated polymer solution. Therefore, the effect of the existence of increasing amount of small size PLLA crystals is seen as multiple melting peaks in the DSC thermogram of porous PLLA scaffolds fabricated at a high-polymer concentration of 5 wt.%.

3.3 Mechanical behavior of PLLA foams

Table 2 compares the brittleness, flexibility, and general aspect of the foams under hand-applied deformations. These mechanical characteristics were assessed with visual aids following techniques reported by Schugens et al. [8, 10]. Scaffolds the size of the glass petridish (diameter of 55 mm) and height of approximately 5 mm were used. Depending on the resistance to pressure, the material was classified as hard or soft. The ability to compress the scaffold to more than 5 mm was considered as soft. The scaffold was considered tough or brittle depending on its response to flexure with a bending displacement of 10 mm

at the sides. Flexibility of scaffolds was grouped according to low, moderate and high with respect to the readiness of the scaffold to be deformed by flexion.

The effect of the initial polymer concentration on the mechanical behavior of the foams is clearly observed. The 1 wt.% solution gave rise to foams which were soft with high flexibility while the higher concentration solutions (3–5 wt.%) gave rigid foams, which were hard and tough.

The foams obtained from the dry ice/ethanol bath had slightly higher flexibility compared to those from freezer at −80°C. The more porous morphology and smaller pore size in the dry ice/ethanol mixture scaffolds would be responsible for the different mechanical properties.

4 Conclusion

From this study, PLLA porous scaffolds were successfully created using a technique known as freeze-extraction that involves phase separation principles without the use of a freeze-dryer. Problems encountered with the use of freeze-dryer like pores in scaffold altered or destroyed during the process of freeze drying to remove the solvent and formation of surface skin due to interfacial tension during the evaporation of the solvent were not met in this study. The use of a different freezing medium, a dry ice/ethanol bath, still permitted the formation of ladder-like structure scaffolds. It was more advantageous to use a dry ice/ethanol bath as it presented a more open scaffold architecture and increased pore interconnectivity. Formation of the ladder-like structure was highly dependent on the initial concentration of PLLA in 1,4-dioxane. No defined ladder-like structure could be observed in 1 wt.% samples. The existence of these structures was also more prominent when the scaffolds were fabricated at a lower freezing temperature of −80°C. In addition to the high interconnectivity, the high porosity values of 90–98% presented here indicated the potential of these porous PLLA scaffolds for tissue engineering applications.

References

1. R. Langer, J.P. Vacanti, Science **260**(5110), 920–926 (1993)
2. R.M. Nerem, A. Sambanis, Tissue Eng. **1**(1), 3–13 (1995)
3. S.N. Bhatia, C.S. Chen, Biomed. Microdevice **2**(2), 131–144 (1999)
4. P.X. Ma, Mater. Today **7**(5), 30–40 (2004)
5. A.G. Mikos, A.J. Thorsen, L.A. Czerwonka, Y. Bao, R. Langer, Polymer **35**(5), 1068–1077 (1994)
6. R.C. Thomson, M.J. Yaszemski, J.M. Powers, A.G. Mikos, Biomaterials **19**(21), 1935–1943 (1998)
7. P.X. Ma, R. Zhang, J. Biomed. Mater. Res. **56**(4), 469–477 (2001)
8. C. Schugens, V. Maquet, C. Grandfils, R. Jerome, P. Teyssie, J. Biomed. Mater. Res. **30**, 449–461 (1996)
9. K. Whang, C.H. Thomas, K.E. Healy, Polymer **36**(4), 837–842 (1995)
10. C. Schugens, V. Maquet, C. Grandfils, R. Jerome, P. Teyssie, Polymer **37**(6), 1027–1038 (1996)
11. C. Tu, Q. Cai, J. Yang, Y. Wan, J. Bei, S. Wang, Polym. Adv. Technol. **14**(8), 565–573 (2003)
12. M.H. Ho, P. Kuo, H. Hsieh, T. Hsien, L. Hou, J. Lai, D. Wang, Biomaterials **25**(1), 129–138 (2004)
13. P.X. Ma, Mater. Today **7**(5), 30–40 (2004)
14. P.X. Ma, in *Scaffolding in Tissue Engineering* (Taylor & Francis, 2006)
15. D.J. Mooney, D.F. Baldwin, N.P. Suht, J.P. Vacantis, R. Langer, Biomaterials **17**(14), 1417–1422 (1996)
16. L.D. Harris, B.S. Kim, D.J. Mooney, J. Biomed. Mater. Res. **42**(3), 396–402 (1998)
17. D.W. Hutmacher, T. Schantz, I. Zein, K.W. Ng, S.H. Teoh, K.C. Tan, J. Biomed. Mater. Res. **55**(2), 203–216 (2001)
18. T.D. Roy, J.L. Simon, J.L. Ricci, E.D. Rekow, V.P. Thompson, J.R. Parsons, J. Biomed. Mater. Res. A **66**(2), 283–291 (2003)
19. V.J. Chen, P.X. Ma, Biomaterials **25**(11), 2065–2073 (2004)
20. R. Zhang, P.X. Ma, J. Biomed. Mater. Res. **52**(2), 430–438 (2000)
21. S. Yang, K.F. Leong, Z. Du, C.K. Chua, Tissue Eng. **7**(6), 679–689 (2001)
22. L.M. Pineda, M. Busing, R.P. Meinig, S. Gogolewskil, J. Biomed. Mater. Res. **31**(3), 385–394 (1996)
23. J.H. Brauker, V.E. Carr-Brendel, L.A. Martinson, J. Crudele, W.D. Johnston, R.C. Johnson, J. Biomed. Mater. Res. **29**(12), 1517–1524 (1995)
24. J.P. Fisher, T.A. Holland, D. Dean, P.S. Engel, A.G. Mikos, J. Biomater. Sci. Polym. Ed. **12**(6), 673–687 (2001)
25. C.L. Jackson, M. T. Shaw, Polymer, **31**(6), 1070–1084 (1990)